Intelligent Reflecting Surface Enhanced User Cooperation in Wireless Powered Communication Networks

Yuan Zheng, Suzhi Bi, Ying Jun Zhang, Zhi Quan, and Hui Wang

***Abstract*—An intelligent reflecting surface (IRS) comprises a massive number of low-cost passive elements that can be controlled to reflect the incident signals into a structured output pattern. In this letter, we consider IRS-assisted user cooperation in a wireless powered communication network (WPCN), where two users harvest wireless energy and transmit information to a common hybrid access point (HAP). In particular, we exploit the use of IRS to enhance the energy efficiency in the wireless energy transfer (WET) phase and the spectral efficiency in the wireless information transmission (WIT) phase. We derive the maximum common (minimum) throughput performance by jointly optimizing the transmit time and power allocations of the two users and the passive array coefficients on reflecting the wireless energy and information signal. Simulation results show that the use of IRS can effectively improve the throughput performance of cooperative transmission in WPCNs.**

***Index Terms*—Wireless powered communications, intelligent reflecting surface, user cooperation, resource allocation.**

I. Introduction

THE CAPACITY of current wireless networks needs exponential increase to meet the rapidly growing demands for high-data-rate multimedia access in the fifth-generation (5G) networks. A variety of wireless technologies have been proposed and investigated in the recent years to improve the spectral efficiency, such as millimetre wave (mmWave) and massive multiple-input multiple-output (mMIMO) technologies. However, these advanced technologies also impose high energy consumption and hardware cost, which hurdle their deployment in practical systems [1]. To address this problem, recently there have been extensive research works on wireless powered communication networks (WPCNs), which use dedicated wireless energy transferring nodes to power the operation of communication devices [2]–[7]. Compared to its conventional battery-powered counterpart, the WPCN has shown its advantages in lowering the operating cost and improving the robustness of communication service especially in low power applications, such as sensor and Internet of Things (IoT) networks.

Recently, intelligent reflecting surface (IRS) has been envisioned as a promising new hardware solution to enhance wireless communication performance [9]. Specifically, the IRS is composed of a large number of low-cost and reconfigurable reflecting elements that can reflect impinging electromagnetic waves with a controllable phase shift using a smart controller. By properly adjusting the phase shifts of the elements of IRS, the reflected signals can be coherently combined with those from other paths at the receiver to maximize the signal strength. In particular, with the recent developments in metasurface technology [8], we are able to reconfigure the phase shifts in real time, thus greatly enhancing the applicability of IRS under wireless fading channel. The application of IRS in WPCNs has the potential to address the inherent problem of low wireless energy transfer efficiency.

There are a few previous studies on the design of IRS-assisted wireless systems [9]–[12]. For instance, [9] considered the transmit power minimization problem with the constraint of the received signal-to-noise ratio (SNR), where active beamforming at the base station (BS) and passive beamforming at the IRS were jointly optimized. The authors in [10] employed a zero-forcing beamforming method to maximize the sum-rate and energy efficiency of a IRS-assisted network. Reference [11] proposed to use a set of distributed IRSs to assist simultaneous wireless information and power transfer (SWIPT) from a multi-antenna AP to multiple information receivers and energy receivers. Considering a more practical case, the authors in [12] aimed at minimizing the transmit power of AP in downlink MISO communications, assisted by an IRS with finite phase resolution. Most of the existing works only adopt IRS in the forward links (FLs) from the BS to the users to enhance the received signal strength. In practice, the reflection of IRS is also applicable to the reverse links (RLs) to improve the spectral efficiency.

In this letter, we consider an IRS-assisted cooperative communications in a two-user WPCN. As shown in Fig. 1, we consider that an HAP broadcasts wireless energy to two WDs in the FLs and receives cooperative information transmission in the RLs. Besides, WD_2 is allowed to relay the message of WD_1 to the HAP. Specifically, during the WET stage, the IRS is used to strengthen the received energy signals from the HAP. During the WIT stage, the IRS assists the transmission from WD_1 to WD_2 and the two WDs to the HAP. With the proposed IRS-assisted cooperation method, we formulate a rate optimization problem that maximizes the minimum throughput of the two WDs by jointly optimizing the transmit time and power allocations of the two WDs and the

Manuscript received January 11, 2020; accepted February 7, 2020. Date of publication February 19, 2020; date of current version June 10, 2020. This work was supported in part by the National Natural Science Foundation of China under Project 61871271 and Project 61622108, in part by the Guangdong Province Pearl River Scholar Funding Scheme 2018, in part by the Foundation of Shenzhen City under Project JCYJ20170818101824392, and in part by the Science and Technology Innovation Commission of Shenzhen under Project 827/000212. The work of Ying Jun Zhang was supported in part by the General Research Fund established by the Research Grants Council of Hong Kong under Project 14208017. The associate editor coordinating the review of this article and approving it for publication was X. Chu. *(Corresponding author: Suzhi Bi.)*

Yuan Zheng, Suzhi Bi, Zhi Quan, and Hui Wang are with the College of Electronics and Information Engineering, Shenzhen University, Shenzhen 518060, China (e-mail: zhyu@szu.edu.cn; bsz@szu.edu.cn; zquan@szu.edu.cn; wanghsz@szu.edu.cn).

Ying Jun Zhang is with the Department of Information Engineering, Chinese University of Hong Kong, Hong Kong (e-mail: yjzhang@ie.cuhk.edu.hk).

Digital Object Identifier 10.1109/LWC.2020.2974721

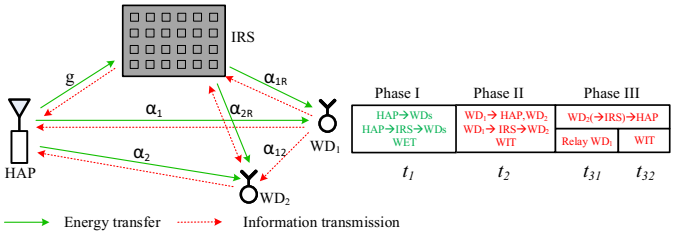

Fig. 1. The considered IRS-aided two-user WPCN system and system time allocation.

passive array coefficients of IRS. Simulation results show that the utilization of IRS can effectively enhance the throughput performance of cooperative transmissions in WPCNs.

II. System Model

As show in Fig. 1, we consider a WPCN consisting of one HAP and two users denoted by WD_1 and WD_2, where the WDs harvest RF energy in the FL and transmit information in the RL. We assume without loss of generality that WD_2 acts as a relay to forward the message of WD_1 to the HAP. It is assumed that each device is equipped with one antenna. To enhance the link performance, an IRS composed of N passive elements is installed on a surrounding wall to assist the transmissions of the WPCN. The IRS can dynamically adjust the phase shift of each reflecting element based on the propagation environment learned through periodic sensing. Due to the substantial path loss, we only consider one-time signal reflection by the IRS and ignore the signals that are reflected thereafter.

We assume that the channel reciprocity holds between the FL and RL and a quasi-static flat fading model for all the channels considered within a time frame of duration T. The channel coefficient vectors of the HAP-to-IRS, IRS-to-WD_i, HAP-to-WD_i and WD_1-to-WD_2 links are denoted as $\mathbf{g} \in \mathbb{C}^{1\times N}$, $\boldsymbol{\alpha}_{iR} \in \mathbb{C}^{N\times 1}, i = 1, 2$, α_i and α_{12}, respectively. We assume that the channels of different transceiver pairs are independent to each other. Besides, the entries inside all channel vectors are modeled as zero-mean independent and identically distributed (i.i.d.) complex Gaussian random variables with variance depending on the path loss of the respective wireless links. The corresponding channel gains are denoted as $g = \|\mathbf{g}\|^2$, $h_{iR} = \|\boldsymbol{\alpha}_{iR}\|^2$, $h_i = |\alpha_i|^2$ and $h_{12} = |\alpha_{12}|^2$. Let $\boldsymbol{\theta} = [\theta_1, \ldots, \theta_N]$ and $\boldsymbol{\Theta} = \mathrm{diag}(\beta_1 e^{j\theta_1}, \ldots, \beta_n e^{j\theta_n}, \ldots, \beta_N e^{j\theta_N})$ (with diag($\mathbf{a}$) denoting a diagonal matrix with its diagonal elements given in the vector $\mathbf{a}$) denote the phase-shift matrix of the IRS, where $\theta_n \in \mathcal{R}$ and $\beta_n \in [0, 1]$ are the phase shift and amplitude reflection coefficient of each element, respectively. In our problem, it is desirable to maximize the signal reflection by the IRS. Thus, we set $\beta_n = 1$ in the following analysis, i.e., $\boldsymbol{\Theta} = \mathrm{diag}(e^{j\theta_1}, \ldots, e^{j\theta_n}, \ldots, e^{j\theta_N})$. We assume that a central control point (such as the HAP) is aware of the channel coefficients $\{\alpha_1, \alpha_2, \alpha_{12}\}$, and coordinates the transmissions of all the devices in the system.[1]

As show in Fig. 1, the system operates in three phases within a time frame. In the first phase of duration t_1, the HAP transfers wireless energy in the FL, while both WDs harvest RF energy. Meanwhile, the IRS scatters the incident signal from the HAP to the WDs, such that the WDs receive both the direct-path and reflect-path signal from the HAP. In the second phase of duration t_2, WD_1 uses the harvested energy to transmit its information to WD_2 in conventional active communication mode. Besides, the IRS reflects the signal of WD_1 to WD_2. In the last phase of length t_3, WD_2 first relays the information of the far user WD_1 to the HAP with transmit power P_{31} over t_{31} amount of time, and then transmits its own information to the HAP with transmit power P_{32} over t_{32} amount of time, respectively, where $t_3 = t_{31} + t_{32}$. Meanwhile, the IRS reflects the signal of WD_2 to the HAP. Note that we have a total time constraint

$$t_1 + t_2 + t_{31} + t_{32} \le T. \tag{1}$$

III. Throughput Performance Analysis

During the first phase, the HAP transmits energy with fixed power P_1 in t_1 amount of time. We denote the energy signal as $x_0(t)$ with $E[|x_0(t)|^2] = 1$. The signal received at WD_i, is then expressed as [9]

$$y_i^{(1)}(t) = (\mathbf{g}\boldsymbol{\Theta}_1\boldsymbol{\alpha}_{iR} + \alpha_i)\sqrt{P_1}x_0(t) + n_i^{(1)}(t), i = 1, 2, \tag{2}$$

where $\boldsymbol{\Theta}_1 = \mathrm{diag}(v_{1,1}, \ldots, v_{1,N})$ denotes the energy reflection coefficient matrix at the IRS. Here $v_{1,n} \triangleq e^{j\theta_{1,n}}$ and $\theta_{1,n}$ denotes the corresponding IRS phase shift for $n = 1, \ldots, N$. Equivalently, we have $|v_{1,n}| = 1, n = 1, \ldots, N$ [16]. $n_1^{(1)}(t)$ and $n_2^{(1)}(t)$ denote the receiver noises. The amount of energy harvested by the i-th WD can be expressed as

$$E_i^{(1)} = \eta E[|y_i^{(1)}(t)|^2]t_1 = \eta|\mathbf{g}\boldsymbol{\Theta}_1\boldsymbol{\alpha}_{iR} + \alpha_i|^2 P_1 t_1, \tag{3}$$

where $0 < \eta < 1$ denotes the fixed energy harvesting efficiency.[2]

Within the following t_2 amount of time, WD_1 uses the harvested energy to transmit its information. Meanwhile, the IRS reflects the information of WD_1 to WD_2. By exhausting its harvested energy on WIT, the transmit power of WD_1 is

$$P_2 = E_1^{(1)}/t_2 = \eta P_1|\mathbf{g}\boldsymbol{\Theta}_1\boldsymbol{\alpha}_{1R} + \alpha_1|^2 t_1/t_2. \tag{4}$$

We denote $x_1(t)$ as the transmitted signal from WD_1 with $E[|x_1(t)|^2] = 1$. The received signals at WD_2 and the HAP during this phase are expressed as

$$y_1^{(2)}(t) = (\boldsymbol{\alpha}_{2R}^T\boldsymbol{\Theta}_2\boldsymbol{\alpha}_{1R} + \alpha_{12})\sqrt{P_2}x_1(t) + n_1^{(2)}(t), \tag{5}$$

$$y_0^{(2)}(t) = (\mathbf{g}\boldsymbol{\Theta}_2\boldsymbol{\alpha}_{1R} + \alpha_1)\sqrt{P_2}x_1(t) + n_0^{(2)}(t), \tag{6}$$

where $\boldsymbol{\Theta}_2 = \mathrm{diag}(v_{2,1}, \ldots, v_{2,N})$ denotes the reflection-coefficient matrix at the IRS with $|v_{2,n}| = 1, n = 1, \ldots, N$, $(\cdot)^T$ denotes the transpose operator, $n_1^{(2)}(t)$ and $n_0^{(2)}(t)$ denote the independent Gaussian receiver noises both with power N_0.

Then, the achievable rates from WD_1 to WD_2 and the HAP in phase II are

$$R_1^{(2)} = \frac{t_2}{T}\log_2\left(1 + \frac{P_2|\boldsymbol{\alpha}_{2R}^T\boldsymbol{\Theta}_2\boldsymbol{\alpha}_{1R} + \alpha_{12}|^2}{N_0}\right), \tag{7}$$

[1]Channel estimation methods for IRS system have been studied in [14] and [15], which is out of the scope of this letter.

[2]Although a single energy harvesting circuit exhibits non-linear energy harvesting property due to the saturation effect of circuit, it is shown that the non-linear effect can be effectively rectified by using multiple energy harvesting circuits concatenated in parallel, resulting in a sufficiently large linear conversion region in practice [17].

$$R_0^{(2)} = \frac{t_2}{T}\log_2\left(1+\frac{P_2|\mathbf{g}\mathbf{\Theta}_2\boldsymbol{\alpha}_{1R}+\alpha_1|^2}{N_0}\right). \quad (8)$$

In the last phase of duration t_3, WD_2 first relays the message of WD_1 and then transmits its own message to the HAP. Meanwhile, the IRS reflects the signal of WD_2 to the HAP. Let $x_{2i}(t)$ denote the transmitted signal for WD_i with $E[|x_{2i}(t)|^2]=1, i=1,2$. Then, the received signal of WD_i at the HAP is

$$y_i^{(3)}(t) = (\mathbf{g}\mathbf{\Theta}_3\boldsymbol{\alpha}_{2R}+\alpha_2)\sqrt{P_{3i}}x_{2i}(t)+n_0^{(3)}(t), i=1,2, \quad (9)$$

where $\mathbf{\Theta}_3 = \mathrm{diag}(v_{3,1},\ldots,v_{3,N})$ denotes the reflection-coefficient matrix at the IRS during phase III with $|v_{3,n}| = 1, n=1,\ldots,N$. The total energy consumption on WD_2 is restricted by the energy harvested in phase I, i.e.,

$$t_{31}P_{31}+t_{32}P_{32} \le E_2^{(1)}. \quad (10)$$

Then, the date rate of WD_2 relaying the information of WD_1 to the HAP is

$$R_1^{(3)} = \frac{t_{31}}{T}\log_2\left(1+\frac{P_{31}|\mathbf{g}\mathbf{\Theta}_3\boldsymbol{\alpha}_{2R}+\alpha_2|^2}{N_0}\right). \quad (11)$$

Overall, the achievable rates of WD_1 and WD_2 are [13]

$$R_1 = \min\left[R_1^{(2)}, R_0^{(2)}+R_1^{(3)}\right], \quad (12)$$

$$R_2 = \frac{t_{32}}{T}\log_2\left(1+\frac{P_{32}|\mathbf{g}\mathbf{\Theta}_3\boldsymbol{\alpha}_{2R}+\alpha_2|^2}{N_0}\right). \quad (13)$$

Without loss of generality, we assume $T=1$ in this letter.

IV. Common Throughput Maximization

In this letter, we are interested in maximizing the common (minimum) throughput of the two WDs by jointly optimizing the phase shift matrices $\mathbf{\Theta}_1$, $\mathbf{\Theta}_2$ and $\mathbf{\Theta}_3$, the transmit time allocation $\mathbf{t} = [t_1, t_2, t_{31}, t_{32}]$ and power allocation $\mathbf{P} = [P_{31}, P_{32}]$, i.e.,

$$\begin{aligned}(\mathrm{P1}): \max_{\mathbf{t},\mathbf{P},\mathbf{\Theta}_1,\mathbf{\Theta}_2,\mathbf{\Theta}_3} \quad & \min(R_1,R_2)\\ \text{s.t.} \quad & (1),\ (3),\ (4)\text{ and }(10),\\ & t_1,t_2,t_{31},t_{32},P_{31},P_{32}\ge 0,\\ & |v_{i,n}|=1, i=1,2,3, n=1,\ldots,N. \quad (14)\end{aligned}$$

(P1) is non-convex in the above form because of the modulus constraint and the multiplicative terms in (3), (4) and (10). To tackle the non-convex problem (P1), we first design the phase shift matrices in phase II and III.

Let $\boldsymbol{v}_i = [v_{i,1},\ldots,v_{i,N}], i=1,2,3$. Then, we have $\mathbf{g}\mathbf{\Theta}_1\boldsymbol{\alpha}_{iR} = \boldsymbol{v}_1\mathrm{diag}(\mathbf{g})\boldsymbol{\alpha}_{iR}, i=1,2$, $\boldsymbol{\alpha}_{2R}^T\mathbf{\Theta}_2\boldsymbol{\alpha}_{1R} = \boldsymbol{v}_2\mathrm{diag}(\boldsymbol{\alpha}_{2R}^T)\boldsymbol{\alpha}_{1R}$ and $\mathbf{g}\mathbf{\Theta}_3\boldsymbol{\alpha}_{2R} = \boldsymbol{v}_3\mathrm{diag}(\mathbf{g})\boldsymbol{\alpha}_{2R}$, such that

$$|\mathbf{g}\mathbf{\Theta}_1\boldsymbol{\alpha}_{iR}+\alpha_i|^2 = |\boldsymbol{v}_1\boldsymbol{\gamma}_i+\alpha_i|^2, i=1,2, \quad (15)$$

$$|\boldsymbol{\alpha}_{2R}^T\mathbf{\Theta}_2\boldsymbol{\alpha}_{1R}+\alpha_{12}|^2 = |\boldsymbol{v}_2\boldsymbol{\gamma}_{12}+\alpha_{12}|^2, \quad (16)$$

$$|\mathbf{g}\mathbf{\Theta}_3\boldsymbol{\alpha}_{2R}+\alpha_2|^2 = |\boldsymbol{v}_3\boldsymbol{\gamma}_2+\alpha_2|^2, \quad (17)$$

where $\boldsymbol{\gamma}_i = \mathrm{diag}(\mathbf{g})\boldsymbol{\alpha}_{iR}, i=1,2$ and $\boldsymbol{\gamma}_{12} = \mathrm{diag}(\boldsymbol{\alpha}_{2R}^T)\boldsymbol{\alpha}_{1R}$. To maximize the signal-to-noise power ratio (SNR) at WD_2, we solve

$$\begin{aligned}(\mathrm{P2}): \max_{\boldsymbol{v}_2} \quad & |\boldsymbol{v}_2\boldsymbol{\gamma}_{12}+\alpha_{12}|\\ \text{s.t.} \quad & |v_{2,n}|=1,\ n=1,\ldots,N. \quad (18)\end{aligned}$$

By the triangle inequality, the objective function of (P2) satisfies the following inequality:

$$|\boldsymbol{v}_2\boldsymbol{\gamma}_{12}+\alpha_{12}| \le \sum_{i=1}^{N}|v_{2,i}[\boldsymbol{\gamma}_{12}]_i|+|\alpha_{12}| = \sum_{i=1}^{N}|[\boldsymbol{\gamma}_{12}]_i|+|\alpha_{12}|, \quad (19)$$

where $[\boldsymbol{\gamma}_{12}]_i$ denotes the *i*-th element of $\boldsymbol{\gamma}_{12}$ and the equality holds because $|v_{2,i}|=1$ for all *i*. Notice that the upper bound in (19) is achievable by setting $\theta_{2,i} = \arg(\alpha_{12})-\arg([\boldsymbol{\gamma}_{12}]_i)$ and $v_{2,i} = e^{j\theta_{2,i}}$ for $i=1,\ldots,N$, where $\arg(\cdot)$ denotes the phase extraction operation. We denote the optimal solution of (P2) as $\boldsymbol{v}_2^*$. Following the similar procedure, we can also obtain the optimal $\boldsymbol{v}_3^*$ in phase III, whose detailed expression is omitted for brevity. Equivalently, we have obtained the optimal $\mathbf{\Theta}_2^*$ and $\mathbf{\Theta}_3^*$ from $\boldsymbol{v}_2^*$ and $\boldsymbol{v}_3^*$, respectively.

Remark 1: From (6), with the optimal phase shift matrix $\mathbf{\Theta}_2^*$ obtained from above, the composite WD_1-HAP channel is $\mathbf{g}\boldsymbol{\mu}+\alpha_1$, where $\boldsymbol{\mu} \triangleq \mathbf{\Theta}_2^*\boldsymbol{\alpha}_{1R}$. By the design of $\mathbf{\Theta}_2^*$, all the entries of $\boldsymbol{\mu}$ are zero-mean i.i.d. complex Gaussian random variables and independent to $\mathbf{g}$. Let $\xi = \frac{\mathbf{g}\boldsymbol{\mu}}{N}$ denote the normalized inner product of $\mathbf{g}$ and $\boldsymbol{\mu}$. According to the asymptotic orthogonality property in massive MIMO channel [18], $\xi \to 0$ when N is very large, resulting in weak reflect-path information signal strength. Therefore, we safely neglect the reflected signal from the IRS to the HAP and consider that the HAP only receives the direct-path signal from WD_1 in phase II.

We continue to optimize $\{\mathbf{\Theta}_1, \mathbf{t}, \mathbf{P}\}$. First, we introduce auxiliary variables $\tau_{31} = t_{31}P_{31}$ and $\tau_{32} = t_{32}P_{32}$. With P_2 in (4), we can express $R_1^{(2)}$ and $R_0^{(2)}$ in (7) and (8), $R_1^{(3)}$ and R_2 in (11) and (13) as

$$R_1^{(2)} = t_2\log_2\left(1+\rho_1|\boldsymbol{v}_1\boldsymbol{\gamma}_1+\alpha_1|^2\frac{t_1}{t_2}\right), \quad (20)$$

$$R_0^{(2)} = t_2\log_2\left(1+\rho_2|\boldsymbol{v}_1\boldsymbol{\gamma}_1+\alpha_1|^2\frac{t_1}{t_2}\right), \quad (21)$$

$$R_1^{(3)} = t_{31}\log_2\left(1+\rho_3\frac{\tau_{31}}{t_{31}}\right), \quad (22)$$

$$R_2 = t_{32}\log_2\left(1+\rho_3\frac{\tau_{32}}{t_{32}}\right), \quad (23)$$

where $\rho_1 = \eta\frac{P_1|\boldsymbol{v}_2^*\boldsymbol{\gamma}_{12}+\alpha_{12}|^2}{N_0}$, $\rho_2 = \eta\frac{P_1h_1}{N_0}$ and $\rho_3 = \frac{|\boldsymbol{v}_3^*\boldsymbol{\gamma}_2+\alpha_2|^2}{N_0}$ are fixed parameters. Thus, (10) can be reformed as

$$\tau_{31}+\tau_{32} \le \eta P_1 t_1|\boldsymbol{v}_1\boldsymbol{\gamma}_2+\alpha_2|^2. \quad (24)$$

Accordingly, by introducing another auxiliary variable $\bar{R}$, we rewrite (P1) as the following problem,

$$\begin{aligned}(\mathrm{P3}): \max_{\overline{R},\mathbf{t},\boldsymbol{v}_1,\boldsymbol{\tau}} \quad & \overline{R}\\ \text{s.t.} \quad & (1)\text{ and }(24),\\ & t_1,t_2,t_{31},t_{32},\tau_{31},\tau_{32}\ge 0,\\ & \overline{R}\le R_0^{(2)}+R_1^{(3)},\\ & \overline{R}\le R_1^{(2)},\ \overline{R}\le R_2,\\ & |v_{1,n}|=1,\ n=1,\ldots,N. \quad (25)\end{aligned}$$

To tackle the non-convex modulus constraint in (P3), we define $\bar{\boldsymbol{v}}_1 = \begin{bmatrix} \boldsymbol{v}_1^T \\ 1 \end{bmatrix}$, $\bar{\boldsymbol{\gamma}}_i = \begin{bmatrix} \boldsymbol{\gamma}_i \\ \alpha_i \end{bmatrix}$, $\mathbf{V}_1 = \bar{\boldsymbol{v}}_1 \bar{\boldsymbol{v}}_1^H$ and $\boldsymbol{\psi}_i = \bar{\boldsymbol{\gamma}}_i \bar{\boldsymbol{\gamma}}_i^H, i = 1, 2$, where $(\cdot)^H$ denotes the complex conjugate operator. Note that $|\boldsymbol{v}_1 \boldsymbol{\gamma}_i + \alpha_i|^2 = \mathrm{tr}(\boldsymbol{\psi}_i \mathbf{V}_1)$, and $[\mathbf{V}_1]_{n,n} = 1, n = 1, \ldots, N+1$ hold from the modulus constraint of $v_{1,n}$ ($[\mathbf{X}]_{m,n}$ denotes the element in the m-th row and n-th column of matrix $\mathbf{X}$). We further define $\mathbf{W} \triangleq t_1 \mathbf{V}_1 \succeq 0$ such that the following condition must hold, i.e.,

$$\mathbf{W}_{n,n} = t_1, n = 1, \ldots, N+1. \tag{26}$$

Therefore, $R_1^{(2)}$ and $R_0^{(2)}$ in (20) and (21), the constraint in (24) can be reformed as, respectively,

$$R_1^{(2)} = t_2 \log_2 \left(1 + \rho_1 \frac{\mathrm{tr}(\boldsymbol{\psi}_1 \mathbf{W})}{t_2}\right), \tag{27}$$

$$R_0^{(2)} = t_2 \log_2 \left(1 + \rho_2 \frac{\mathrm{tr}(\boldsymbol{\psi}_1 \mathbf{W})}{t_2}\right), \tag{28}$$

$$\tau_{31} + \tau_{32} \leq \eta P_1 \mathrm{tr}(\boldsymbol{\psi}_2 \mathbf{W}). \tag{29}$$

Note that $\mathbf{W}$ needs to satisfy $\mathbf{W} \succeq 0$ and $\mathrm{rank}(\mathbf{W}) = 1$. Since the rank-one constraint is non-convex, we drop this constraint and convert (P3) into

$$\begin{aligned} (\mathrm{P4}): \max_{\overline{R}, \mathbf{t}, \boldsymbol{\tau}, \mathbf{W}} \quad & \overline{R} \\ \text{s.t.} \quad & (1), (26) \text{ and } (29), \mathbf{W} \succeq 0, \\ & t_1, t_2, t_{31}, t_{32}, \tau_{31}, \tau_{32} \geq 0, \\ & \overline{R} \leq R_0^{(2)} + R_1^{(3)}, \\ & \overline{R} \leq R_1^{(2)}, \ \overline{R} \leq R_2. \end{aligned} \tag{30}$$

(P4) is a standard semidefinite programming (SDP) and can be optimally solved by convex tools such as CVX [20]. Let us denote the optimal solution to (P4) as $\{\overline{R}^*, \mathbf{t}^*, \boldsymbol{\tau}^*, \mathbf{W}^*\}$, we can obtain the optimal $\mathbf{V}_1^* = \mathbf{W}^*/t_1^*, P_{3i}^* = \tau_{3i}^*/t_{3i}^*, i = 1, 2$. However, the relaxed problem (P4) may not lead to a rank-one solution in general. To recover $\bar{\boldsymbol{v}}_1$ from $\mathbf{V}_1^*$, we follow [9] to obtain the eigenvalue decomposition of $\mathbf{V}_1^*$ as $\mathbf{V}_1^* = \mathbf{U}\boldsymbol{\Sigma}\mathbf{U}^H$, where $\boldsymbol{U} \in \mathbb{C}^{(N+1)\times(N+1)}$ and $\boldsymbol{\Sigma} \in \mathbb{C}^{(N+1)\times(N+1)}$ are a unitary matrix and a diagonal matrix, respectively. Then, we obtain a suboptimal solution as $\bar{\boldsymbol{v}}_1 = \mathbf{U}\boldsymbol{\Sigma}^{1/2}\boldsymbol{r}$, where $\boldsymbol{r} \in \mathbb{C}^{(N+1)\times 1}$ is a random vector with $\boldsymbol{r} \sim \mathcal{CN}(\mathbf{0}, \boldsymbol{I}_{N+1})$. Finally, we have $\theta_{1,i} = \arg([\bar{\boldsymbol{v}}_1]_i)$ and $v_{1,i} = e^{j\theta_{1,i}}$ for $i = 1, \ldots, N$. The optimal $\boldsymbol{\Theta}_1^*$ can be obtained from $\boldsymbol{v}_1^*$.

V. Simulation Results

In this section, we provide simulation results to evaluate the performance of the proposed IRS-assisted cooperation scheme. In all simulations, we set $P_1 = 30$ dBm, $\eta = 0.8$, and $N_0 = -90$ dBm. The distance-dependent path loss model is given by $L = C_0(\frac{d_i}{d_0})^{-\lambda}$, where $C_0 = 30$ dB is the path loss at the reference distance $d_0 = 1$m, $d_i, i = 1, 2$, and d_{12} denote the HAP-WD$_i$ and WD$_1$-WD$_2$ distance, and λ denotes the path loss exponent. To account for small-scale fading, we assume all channels follow Rayleigh fading. To account for heterogeneous channel conditions, we set different path loss exponents of the HAP-IRS, IRS-WD$_i$, HAP-WD$_i$, WD$_1$-WD$_2$ channels as 2.0, 2.5, 3.5, 3.5, respectively. All the simulation results are obtained by averaging over 1000 channel realizations.

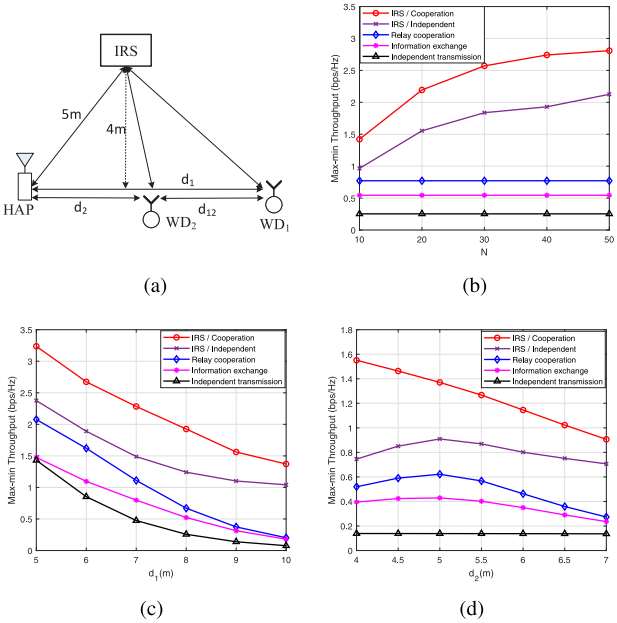

Fig. 2. (a) The placement model of simulation setup. (b) Max-min throughput versus N. (c) Max-min throughput versus d_1. (d) Max-min throughput versus d_2.

For performance comparison, we consider the following representative benchmark methods:

1) Independent transmission with IRS: This method follows the harvest-then-transmit protocol in [3]. Specifically, IRS is used to reflect RF energy from the HAP in FL and the information of WDs in RL.
2) Independent transmission without IRS: WDs transmit their information independently in a round-robin manner to the HAP.
3) Cooperation without IRS: This corresponds to the two-user cooperation method in [13].
4) Cooperation with information exchange (without IRS): This corresponds to the method in [19]. The detailed expressions are omitted here due to the page limit.

For fair comparison, we optimize the resource allocations in all the benchmark schemes, where the details are omitted due to the page limit.

We consider the placement model of the network system in Fig. 2(a). Fig. 2(b) shows the impact of numbers of reflecting elements N to the throughput performance. Without loss of generality, we set $d_1 = 8$ m, $d_2 = 5$ m and $d_{12} = 3$ m, and change the value of N from 10 to 50. Obviously, the two IRS-assisted transmission methods achieve higher throughput due to the array gain. On average, the proposed IRS-assisted cooperation method achieves 40.53%, 204.31%, 264.55% and 652.02% higher throughput than the four benchmark methods, respectively.

Fig. 2(c) shows the impact of the HAP-to-WD$_1$ channel h_1 to the throughput performance. Here, we fix $d_2 = 3$ m, $N = 20$ and vary d_1 from 5 to 10 meters. Notice that the two IRS-assisted communication methods always outperform the other three methods without IRS. Meanwhile, the performance gap between the two IRS-assisted methods gradually decreases with d_1. This shows that a weaker inter-user channel (larger d_1) leads to less efficient cooperation between the two users.

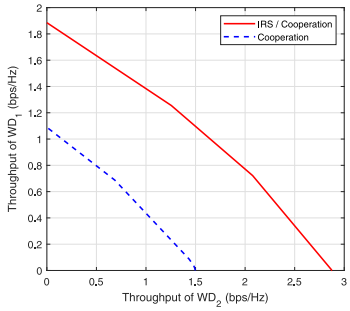

Fig. 3. The achievable rate region comparison of two different methods.

Nonetheless, there exists significant performance gap between the two cooperation methods either with or without the use of IRS, indicating the effective performance enhancement of IRS in both energy and information transmissions.

Fig. 2(d) investigates the throughput performance versus the relaying channel h_2. We set $d_1 = 9$ m, $N = 20$ and vary d_2 from 4 to 7 meters. We first observe that the throughput of the independent transmission method is almost unchanged when d_2 increases, because the performance bottleneck is the weak channel h_1 of the far user WD_1. Similarly, we can see the evident advantage of the two IRS-assisted communication methods. Furthermore, it is observed that the throughput of IRS-assisted independent transmission method and two cooperation without IRS methods first increase when $d_2 < 5$ m, but decrease as d_2 further increases. This is because for the two cooperation without IRS schemes, a larger d_2 improves the inter-user channel initially. For the independent transmission with IRS, a larger d_2 will initially increase the harvested energy of the two users as they get closer. However, as we further increase d_2, we may eventually suffer from very weak WD_2-to-HAP channel. Besides, the performance gap between the two IRS-assisted methods is relatively small when d_2 is large, because the WD_2-to-HAP channel becomes the performance bottleneck for both methods, while the use of cooperation becomes less significant.

Fig. 3 compares the achievable rate regions of two different schemes, i.e., the proposed IRS-assisted cooperation and cooperation without IRS. The rate region can be obtained by replacing the objective of problem (P1) with the weighted sum rate of the two users, i.e., $\omega R_1 + (1-\omega)R_2$, and solve the optimization under different weighting factor ω from 0 to 1. The details are omitted due to the page limit. Here, we set $d_1 = 8$ m, $d_2 = 5$ m, $d_{12} = 3$ m and $N = 20$. Intuitively, we see that the rate region of the proposed IRS-assisted cooperation method is significantly larger than that of the cooperation without IRS scheme. On average, the proposed IRS-assisted cooperation method achieves 74.07% and 91.85% higher throughput for WD_1 and WD_2 than the cooperation without IRS method, respectively.

VI. Conclusion and Future Work

In this letter, we investigated the use of IRS in assisting the transmissions in a two-user cooperative WPCN. We studied the common throughput maximization problem and jointly optimized the phase shifts of the IRS, the transmission time and power allocations. Numerical results verified that the use of IRS can effectively improve the throughput performance of cooperative transmissions in WPCNs. In the future, we may extend this letter to a multi-user WPCN, where one of the users is allowed to relay the information of the other users, or multiple users can share their harvested energy to transmit the information of each other. Moreover, it is also more practical yet challenging to consider a discrete-phase IRS-assisted user cooperation in WPCNs.

References

[1] S. Zhang, Q. Wu, S. Xu, and G. Y. Li, "Fundamental green tradeoffs: Progresses, challenges, and impacts on 5G networks," *IEEE Commun. Surveys Tuts.*, vol. 19, no. 1, pp. 33–56, 1st Quart., 2017

[2] S. Bi, C. K. Ho, and R. Zhang, "Wireless powered communication: Opportunities and challenges," *IEEE Commun. Mag.*, vol. 53, no. 4, pp. 117–125, Apr. 2015.

[3] H. Ju and R. Zhang, "Throughput maximization in wireless powered communication networks," *IEEE Trans. Wireless Commun.*, vol. 13, no. 1, pp. 418–428, Jan. 2014.

[4] S. Bi and Y. J. Zhang, "Computation rate maximization for wireless powered mobile-edge computing with binary computation offloading," *IEEE Trans. Wireless Commun.*, vol. 17, no. 6, pp. 4177–4190, Jun. 2018.

[5] L. Huang, S. Bi, and Y. J. Zhang, "Deep reinforcement learning for online computation offloading in wireless powered mobile-edge computing networks," *IEEE Trans. Mobile Comput.*, early access, doi: 10.1109/TMC.2019.2928811.

[6] Y. Zheng, S. Bi, X. Lin, and H. Wang, "Reusing wireless power transfer for backscatter-assisted relaying in WPCNs," 2019. [Online]. Available: arxiv.org/abs/1912.11623.

[7] L. Yuan, S. Bi, X. Lin, and H. Wang, "Optimizing throughput fairness of cluster-based cooperation in underlay cognitive WPCNs," *Comput. Netw.*, vol. 166, pp. 1–9, Jan. 2020.

[8] T. J. Cui, M. Q. Qi, X. Wan, J. Zhao, and Q. Cheng, "Coding metamaterials, digital metamaterials and programmable metamaterials," *Light Sci. Appl.*, vol. 3, no. 10, p. e218, Oct. 2014.

[9] Q. Wu and R. Zhang, "Intelligent reflecting surface enhanced wireless network via joint active and passive beamforming," *IEEE Trans. Wireless Commun.*, vol. 18, no. 11, pp. 5394–5409, Nov. 2019.

[10] C. Huang, A. Zappone, M. Debbah, and C. Yuen, "Achievable rate maximization by passive intelligent mirrors," in *Proc. IEEE Int. Conf. Acoust. Speech Signal Process. (ICASSP)*, Calgary, AB, Canada, May 2018, pp. 3714–3718.

[11] Q. Wu and R. Zhang, "Joint active and passive beamforming optimization for intelligent reflecting surface assisted SWIPT under QOS constraints," 2019. [Online]. Available: arxiv.org/abs/1910.06220.

[12] Q. Wu and R. Zhang, "Beamforming optimization for wireless network aided by intelligent reflecting surface with discrete phase shifts," *IEEE Trans. Commun.*, early access, doi: 10.1109/TCOMM.2019.2958916.

[13] H. Ju and R. Zhang, "User cooperation in wireless powered communication networks," in *Proc. IEEE Global Commun. Conf. (GLOBECOM)*, Austin, TX, USA, Dec. 2014, pp. 1430–1435.

[14] D. Mishra and H. Johansson, "Channel estimation and low-complexity beamforming design for passive intelligent surface assisted MISO wireless energy transfer," in *Proc. IIEEE Int. Conf. Acoust. Speech Signal Process. (ICASSP)*, Brighton, U.K., May 2019, pp. 4659–4663.

[15] Q. U.-A. Nadeem, A. Kammoun, A. Chaaban, M. Debbah, and M.-S. Alouini, "Intelligent reflecting surface assisted multi-user MISO communication," 2019. [Online]. Available: arxiv.org/abs/1906.02360.

[16] C. Huang, A. Zappone, G. C. Alexandropoulos, M. Debbah, and C. Yuen, "Reconfigurable intelligent surfaces for energy efficiency in wireless communication," *IEEE Trans. Wireless Commun.*, vol. 18, no. 8, pp. 4157–4170, Aug. 2019.

[17] J. M. Kang, I. M. Kim, and D. I. Kim, "Joint Tx power allocation and Rx power splitting for SWIPT system with multiple nonlinear energy harvesting circuit," *IEEE Wireless Commun. Lett.*, vol. 8, no. 1, pp. 53–56, Feb. 2019.

[18] F. Rusek *et al.*, "Scaling up MIMO: Opportunities and challenges with very large arrays," *IEEE Signal Process. Mag.*, vol. 30, no. 1, pp. 40–60, Jan. 2013.

[19] M. Zhong, S. Bi, and X. Lin, "User cooperation for enhanced throughput fairness in wireless powered communication networks," *Wireless Netw.*, vol. 23, no. 4, pp. 1315–1330, Apr. 2017.

[20] S. Boyd and L. Vandenberghe, *Convex Optimization*. Cambridge, U.K.: Cambridge Univ. Press, 2004.